

Observation of the decay $\bar{B}^0 \rightarrow D_s^+ \Lambda \bar{p}$

T. Medvedeva,¹ R. Chistov,¹ K. Abe,² K. Abe,³ I. Adachi,² H. Aihara,⁴ D. Anipko,⁵ T. Aushev,^{6,1} A. M. Bakich,⁷ V. Balagura,¹ E. Barberio,⁸ A. Bay,⁶ K. Belous,⁹ U. Bitenc,¹⁰ I. Bizjak,¹⁰ A. Bondar,⁵ A. Bozek,¹¹ M. Bračko,^{2,12,10} J. Brodzicka,¹¹ T. E. Browder,¹³ M.-C. Chang,¹⁴ P. Chang,¹⁵ Y. Chao,¹⁵ A. Chen,¹⁶ W. T. Chen,¹⁶ B. G. Cheon,¹⁷ Y. Choi,¹⁸ Y. K. Choi,¹⁸ S. Cole,⁷ J. Dalseno,⁸ M. Danilov,¹ M. Dash,¹⁹ A. Drutskoy,²⁰ S. Eidelman,⁵ S. Fratina,¹⁰ N. Gabyshev,⁵ A. Garmash,²¹ T. Gershon,² A. Go,¹⁶ B. Golob,^{22,10} H. Ha,²³ J. Haba,² K. Hayasaka,²⁴ H. Hayashii,²⁵ M. Hazumi,² D. Heffernan,²⁶ T. Hokuue,²⁴ Y. Hoshi,³ S. Hou,¹⁶ W.-S. Hou,¹⁵ T. Iijima,²⁴ A. Imoto,²⁵ K. Inami,²⁴ A. Ishikawa,⁴ R. Itoh,² M. Iwasaki,⁴ Y. Iwasaki,² J. H. Kang,²⁷ H. Kawai,²⁸ T. Kawasaki,²⁹ H. R. Khan,³⁰ H. Kichimi,² Y. J. Kim,³¹ P. Krokovny,² R. Kulasiri,²⁰ R. Kumar,³² C. C. Kuo,¹⁶ Y.-J. Kwon,²⁷ G. Leder,³³ M. J. Lee,³⁴ S. E. Lee,³⁴ T. Lesiak,¹¹ S.-W. Lin,¹⁵ D. Liventsev,¹ G. Majumder,³⁵ F. Mandl,³³ T. Matsumoto,³⁶ S. McOnie,⁷ W. Mitaroff,³³ H. Miyake,²⁶ H. Miyata,²⁹ Y. Miyazaki,²⁴ R. Mizuk,¹ G. R. Moloney,⁸ T. Mori,²⁴ Y. Nagasaka,³⁷ M. Nakao,² Z. Natkaniec,¹¹ S. Nishida,² O. Nitoh,³⁸ S. Ogawa,³⁹ T. Ohshima,²⁴ S. Okuno,⁴⁰ Y. Onuki,⁴¹ H. Ozaki,² P. Pakhlov,¹ G. Pakhlova,¹ H. Park,⁴² K. S. Park,¹⁸ L. S. Peak,⁷ R. Pestotnik,¹⁰ L. E. Piilonen,¹⁹ H. Sahoo,¹³ Y. Sakai,² N. Satoyama,⁴³ T. Schietinger,⁶ O. Schneider,⁶ R. Seidl,^{44,41} K. Senyo,²⁴ M. E. Sevir,⁸ M. Shapkin,⁹ H. Shibuya,³⁹ J. B. Singh,³² A. Sokolov,⁹ A. Somov,²⁰ N. Soni,³² S. Stanič,⁴⁵ M. Starič,¹⁰ H. Stoeck,⁷ T. Sumiyoshi,³⁶ F. Takasaki,² K. Tamai,² M. Tanaka,² G. N. Taylor,⁸ Y. Teramoto,⁴⁶ X. C. Tian,⁴⁷ I. Tikhomirov,¹ T. Tsuboyama,² T. Tsukamoto,² S. Uehara,² T. Uglov,¹ K. Ueno,¹⁵ Y. Unno,¹⁷ S. Uno,² P. Urquijo,⁸ Y. Usov,⁵ G. Varner,¹³ S. Villa,⁶ C. C. Wang,¹⁵ C. H. Wang,⁴⁸ Y. Watanabe,³⁰ E. Won,²³ Q. L. Xie,⁴⁹ A. Yamaguchi,⁵⁰ Y. Yamashita,⁵¹ M. Yamauchi,² Z. P. Zhang,⁵² and A. Zupanc¹⁰

(The Belle Collaboration)

¹*Institute for Theoretical and Experimental Physics, Moscow*

²*High Energy Accelerator Research Organization (KEK), Tsukuba*

³*Tohoku Gakuin University, Tagajo*

⁴*Department of Physics, University of Tokyo, Tokyo*

⁵*Budker Institute of Nuclear Physics, Novosibirsk*

⁶*Swiss Federal Institute of Technology of Lausanne, EPFL, Lausanne*

⁷*University of Sydney, Sydney NSW*

⁸*University of Melbourne, Victoria*

⁹*Institute of High Energy Physics, Protvino*

¹⁰*J. Stefan Institute, Ljubljana*

¹¹*H. Niewodniczanski Institute of Nuclear Physics, Krakow*

¹²*University of Maribor, Maribor*

¹³*University of Hawaii, Honolulu, Hawaii 96822*

¹⁴*Department of Physics, Fu Jen Catholic University, Taipei*

¹⁵*Department of Physics, National Taiwan University, Taipei*

¹⁶*National Central University, Chung-li*

¹⁷*Hanyang University, Seoul*

¹⁸*Sungkyunkwan University, Suwon*

¹⁹*Virginia Polytechnic Institute and State University, Blacksburg, Virginia 24061*

²⁰*University of Cincinnati, Cincinnati, Ohio 45221*

²¹*Princeton University, Princeton, New Jersey 08544*

²²*University of Ljubljana, Ljubljana*

²³*Korea University, Seoul*

²⁴*Nagoya University, Nagoya*

²⁵*Nara Women's University, Nara*

²⁶*Osaka University, Osaka*

²⁷*Yonsei University, Seoul*

²⁸*Chiba University, Chiba*

²⁹*Niigata University, Niigata*

³⁰*Tokyo Institute of Technology, Tokyo*

³¹*The Graduate University for Advanced Studies, Hayama, Japan*

³²*Panjab University, Chandigarh*

³³*Institute of High Energy Physics, Vienna*

³⁴*Seoul National University, Seoul*

³⁵*Tata Institute of Fundamental Research, Bombay*

³⁶*Tokyo Metropolitan University, Tokyo*

³⁷*Hiroshima Institute of Technology, Hiroshima*

³⁸*Tokyo University of Agriculture and Technology, Tokyo*

³⁹*Toho University, Funabashi*

⁴⁰*Kanagawa University, Yokohama*

⁴¹*RIKEN BNL Research Center, Upton, New York 11973*

⁴²*Kyungpook National University, Taegu*

⁴³*Shinshu University, Nagano*

⁴⁴*University of Illinois at Urbana-Champaign, Urbana, Illinois 61801*

⁴⁵*University of Nova Gorica, Nova Gorica*

⁴⁶*Osaka City University, Osaka*

⁴⁷*Peking University, Beijing*

⁴⁸*National United University, Miao Li*

⁴⁹*Institute of High Energy Physics, Chinese Academy of Sciences, Beijing*

⁵⁰*Tohoku University, Sendai*

⁵¹*Nippon Dental University, Niigata*

⁵²*University of Science and Technology of China, Hefei*

We report the first observation of the decay $\bar{B}^0 \rightarrow D_s^+ \Lambda \bar{p}$ with a statistical significance of 6.6σ . We measure $\mathcal{B}(\bar{B}^0 \rightarrow D_s^+ \Lambda \bar{p}) = (2.9 \pm 0.7 \pm 0.5 \pm 0.4) \times 10^{-5}$, where the first error is statistical, the second is systematic and the third error comes from the uncertainty in $\mathcal{B}(D_s^+ \rightarrow \phi \pi^+)$. The data used for this analysis was accumulated at the $\Upsilon(4S)$ resonance, using the Belle detector at the KEKB asymmetric-energy e^+e^- collider. The integrated luminosity of the data sample is 414 fb^{-1} , corresponding to $449 \times 10^6 B\bar{B}$ pairs.

PACS numbers: 13.25.Hw, 13.30.Eg, 14.40.Lb, 14.20.Jn

In the past few years, new measurements of baryonic B meson decays by Belle [1, 2, 3, 4, 5] and CLEO [6, 7] have revived experimental [8, 9, 10] and theoretical interest [11, 12, 13, 14, 15, 16] in such processes. Multi-body baryonic decay modes are found to have larger branching fractions than two-body modes, and the baryon-pair invariant mass spectrum peaks near threshold in the case of multi-body decays [17]. This feature was conjectured in Ref. [18]. Further investigations of the Dalitz plot [19] and the angular correlations for events in the threshold region [20] offer better understanding of the underlying dynamics.

To date, nothing is known experimentally about charmful baryonic B decays with the creation of an $s\bar{s}$ pair. \bar{B}^0 mesons can decay to $D_s^+ \Lambda \bar{p}$ through the Cabibbo favoured $b \rightarrow \bar{c}ud$ process. They can also decay to the charge conjugate final state through the Cabibbo suppressed $b \rightarrow u\bar{c}d$ process, opening a new avenue for future CP asymmetry studies. We report here the first observation of the decay $\bar{B}^0 \rightarrow D_s^+ \Lambda \bar{p}$ using 414 fb^{-1} of data, corresponding to $449 \times 10^6 B\bar{B}$ pairs, collected at the $\Upsilon(4S)$ resonance with the Belle detector at the KEKB asymmetric-energy e^+e^- collider [21]. Since the $D_s^+ \Lambda \bar{p}$ final state may get a contribution from the $D^0 p \rightarrow D_s^+ \Lambda$ final state rescattering, the previously observed $B^0 \rightarrow D^0 p \bar{p}$ decay [5] could be one of the sources for the $D_s^+ \Lambda \bar{p}$ final state. Inclusion of charge conjugate states is implicit throughout this paper.

The Belle detector is a large-solid-angle magnetic spectrometer that consists of a silicon vertex detector (SVD), a 50-layer central drift chamber (CDC), an array of aerogel threshold Cherenkov counters (ACC), a barrel-like arrangement of time-of-flight scintillation counters

(TOF), and an electromagnetic calorimeter (ECL) comprised of CsI(Tl) crystals located inside a superconducting solenoid coil that provides a 1.5 T magnetic field. An iron flux-return located outside the coil is instrumented to detect K_L^0 mesons and to identify muons (KLM). The detector is described in detail elsewhere [22]. Two different inner detector configurations were used. For the first sample of 152 million $B\bar{B}$ pairs, a 2.0 cm radius beampipe and a 3-layer silicon vertex detector were used; for the latter 297 million $B\bar{B}$ pairs, a 1.5 cm radius beampipe, a 4-layer silicon detector and a small-cell inner drift chamber were used [23]. We use a GEANT-based Monte Carlo (MC) simulation to model the response of the detector and determine the efficiency [24].

Pions, kaons and protons are identified using a likelihood ratio method, which combines information from the TOF system and ACC counters with dE/dx measurements using the CDC [25].

In this analysis we reconstruct D_s^+ candidates by using $D_s^+ \rightarrow \phi \pi^+$, $\bar{K}^{*0} K^+$ and $K_S^0 K^+$ decay modes. Candidate Λ baryons are reconstructed via the $\Lambda \rightarrow p \pi^-$ decay.

For Λ hyperons we require an invariant mass within $\pm 3 \text{ MeV}/c^2$ of the nominal Λ mass [26]. The distance between the Λ decay vertex position and beam interaction point (IP) in the $r - \phi$ plane, $dr(\Lambda)$, is required to be greater than 0.5 cm. The angle α_Λ , between the Λ momentum vector and the vector pointing from the IP to the decay vertex, must satisfy $\cos \alpha_\Lambda > 0.95$. We also require $dz(\Lambda) < 0.5 \text{ cm}$, where $dz(\Lambda)$ is the difference in the z -coordinates (the z axis is parallel to the e^+ beam) between the π and p tracks at vertex position. We reconstruct neutral kaons via the decay $K_S^0 \rightarrow \pi^+ \pi^-$ and require its invariant mass to be within

$\pm 10 \text{ MeV}/c^2$ (about 4σ) of the nominal K_S^0 mass. We also require $dz(K_S^0) < 1 \text{ cm}$, $dr(K_S^0) > 0.01 \text{ cm}$ and $|\cos(\alpha_{K_S^0})| > 0.95$, where dz , dr and α are defined in a way similar to the case of the Λ hyperon.

We use a mass and vertex constrained fit for $D_s^+ \rightarrow K^+ K^- \pi^+$, and require the ϕ invariant mass to be within $\pm 10 \text{ MeV}/c^2$ and \bar{K}^{*0} invariant mass within $\pm 50 \text{ MeV}/c^2$ of the nominal masses for the $D_s^+ \rightarrow \phi \pi^+$ and $D_s^+ \rightarrow \bar{K}^{*0} K^+$, respectively. Finally, we apply helicity requirements: $|\cos \Theta_\phi| > 0.3$ and $|\cos \Theta_{\bar{K}^{*0}}| > 0.3$ for $D_s^+ \rightarrow \phi \pi$ and $D_s^+ \rightarrow \bar{K}^{*0} K^+$, respectively. The helicity angle $\Theta_{\phi(K^*)}$ is defined as the angle between the $K(\pi)$ meson momentum and the D_s meson momentum in the $\phi(K^*)$ rest frame. For D_s candidates we use a mass window that extends $\pm 15 \text{ MeV}/c^2$ around the nominal D_s mass value. We use a large sample of inclusive Λ and D_s signals, applying the selections described above, to verify that their mass peaks are well described by two Gaussians, corresponding to the core and the tail of the distribution, where the tail fraction is 35 to 50%. The signal mass windows that are used in the analysis correspond to approximately 4σ for the core and 2σ for the tail Gaussian. For the inclusive signals data and MC agree.

To suppress the continuum background ($e^+e^- \rightarrow q\bar{q}$, where $q = u, d, s, c$), we require the ratio of the second to zeroth Fox-Wolfram moment [27] to be less than 0.5. We also require the cosine of the reconstructed B meson direction with respect to the z -axis in center-of-mass (c.m.) frame, $|\cos \theta_B|$, to be less than 0.8.

The B candidates are identified by their mass difference, $\Delta M = M(B) - m_B$ and their beam-energy constrained mass, $M_{bc} = \sqrt{E_{\text{beam}}^2 - (\sum_i \vec{p}_i)^2}$, where $E_{\text{beam}} = \sqrt{s}/2$ is the beam energy and \vec{p}_i are three-momenta of the B candidate decay products in the c.m. system, $M(B)$ is the reconstructed mass of the B candidate and m_B is the world average B meson mass. We do not use the widely applied kinematic variable $\Delta E = E_B - E_{\text{beam}}$, where E_B is the energy of the reconstructed B in the c.m. system, since ΔE has a large correlation with M_{bc} for signal due to the small energy release in the decay under study. By contrast, ΔM and M_{bc} are uncorrelated [28, 29] as confirmed by MC. We select B candidates with $M_{bc} > 5.2 \text{ GeV}/c^2$ and $|\Delta M| < 0.2 \text{ GeV}/c^2$.

The M_{bc} and ΔM distributions for the $\bar{B}^0 \rightarrow D_s^+ \Lambda \bar{p}$ candidates are shown in Fig. 1 (a) and (b), respectively, where all three D_s modes are combined. We require $M_{bc} > 5.272 \text{ GeV}/c^2$ ($|\Delta M| < 0.025 \text{ GeV}/c^2$) for the ΔM (M_{bc}) projection. We found that after applying all the selection requirements, there are no events counted repeatedly in the M_{bc} and ΔM distributions. The hatched histograms in Fig. 1 (a) and (b) show normalized D_s mass sidebands where no peaking structures are evident. The superimposed curves are the results of a simultaneous two-dimensional binned maximum likelihood

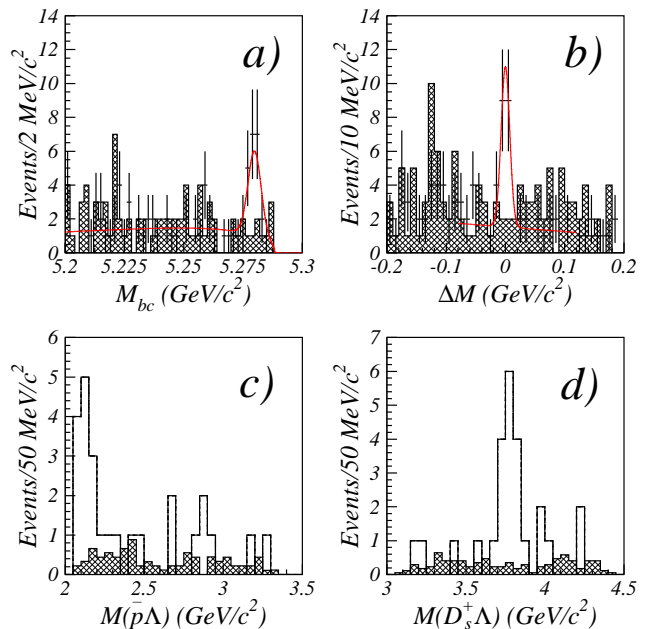


FIG. 1: (a) The M_{bc} and (b) ΔM distributions for the $\bar{B}^0 \rightarrow D_s^+ \Lambda \bar{p}$ candidates (triangles with error bars). The hatched histograms show the D_s^+ mass sidebands normalized to the signal region. The overlaid curves are fit results (see text for details). (c) The $\bar{p}\Lambda$ and (d) $D_s^+ \Lambda$ invariant mass distributions in the B -signal region (open histogram) and in the B -sideband (hatched histogram).

fit (with common branching fraction as a constraint) to the three ΔM versus M_{bc} distributions (for the three D_s channels).

To describe the signal we use Gaussians with means and widths fixed to the values obtained from MC. The backgrounds in M_{bc} and ΔM are parameterized by a first-order polynomial and an ARGUS function [30], respectively. The fit gives a statistical significance of 6.6σ for the signal, where the statistical significance is defined as $\sqrt{-2 \ln(L_0/L_{\text{max}})}$, where L_0 and L_{max} are the likelihoods with the signal fixed at zero and at fitted value, respectively. The region $\Delta M < -0.08 \text{ GeV}/c^2$ is excluded from the fit to avoid possible contributions from the $\bar{B}^0 \rightarrow D_s^{*+} \Lambda \bar{p}$, $D_s^{*+} \rightarrow D_s^+ \gamma$ and $B^- \rightarrow D_s^+ \Lambda \bar{p} \pi^-$ decays, where the soft $\gamma(\pi^-)$ is undetected. The choice of the fitting range is taken into account in the systematic error. The results of the fit applied for the three D_s^+ modes separately are shown in Table I.

We select events in the B -signal region of $|\Delta M| < 0.025 \text{ GeV}/c^2$ and $M_{bc} > 5.272 \text{ GeV}/c^2$ for the three D_s^+ modes and examine the two-baryon invariant mass distribution (Fig. 1 (c)). We see apparent threshold peaking behavior of this distribution, while the B -sideband [31] distribution is smooth. Such a threshold peaking behavior seems intrinsic to all multi-body baryonic B decays.

TABLE I: Summary of the fit results, efficiencies, statistical significances and branching fractions obtained from the 2D $\Delta M - M_{bc}$ fit.

Decay Mode	Yield	Efficiency (10^{-4})	Significance	\mathcal{B} (10^{-5})
$\bar{B}^0 \rightarrow D_s^+ \Lambda \bar{p}, D_s^+ \rightarrow \phi \pi^+$	6.5 ± 2.6	4.90	4.7σ	3.0 ± 1.2
$\bar{B}^0 \rightarrow D_s^+ \Lambda \bar{p}, D_s^+ \rightarrow \bar{K}^{*0} K^+$	4.0 ± 2.5	4.31	2.3σ	2.1 ± 1.3
$\bar{B}^0 \rightarrow D_s^+ \Lambda \bar{p}, D_s^+ \rightarrow K_S^0 K^+$	7.9 ± 3.1	4.83	4.2σ	3.6 ± 1.4
$\bar{B}^0 \rightarrow D_s^+ \Lambda \bar{p}$, simultaneous fit			6.6σ	2.9 ± 0.7

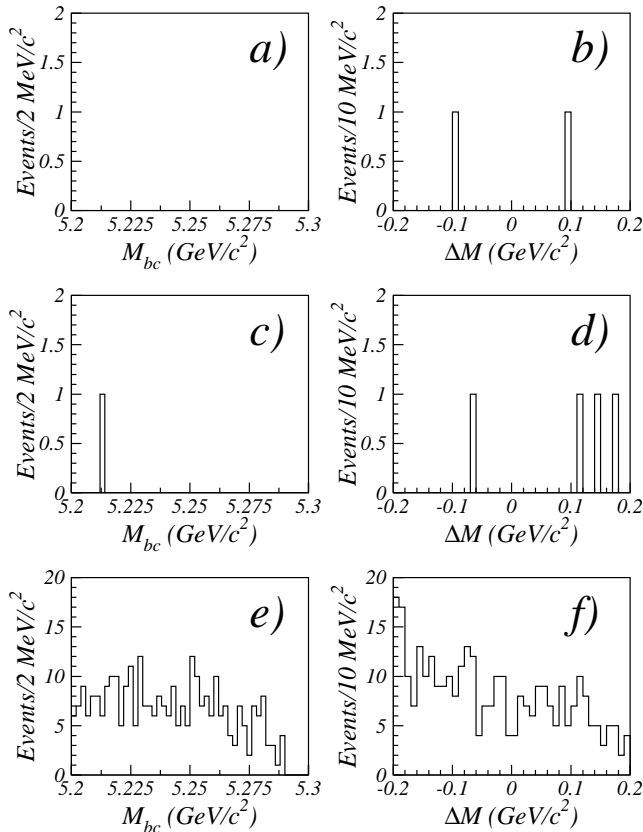


FIG. 2: Cross-checks of the signal. (a) and (b) are the M_{bc} and ΔM distributions for the on-resonance data with the inverted requirement on the normalized Fox-Wolfram moment R_2 (see text for details). (c) and (d) are the M_{bc} and ΔM distributions for the continuum data. (e) and (f) are the M_{bc} and ΔM distributions for the primary vertex protons with inverted identification. No peaking structure in the signal region is present in any of the cross-check analyses.

The invariant mass distribution for D_s^+ and Λ and for corresponding B -sideband is represented as well (Fig. 1 (d)). Some peaking behavior is also seen in this distribution, which could arise from some new excited charm baryon. Firm conclusions, however, cannot yet be drawn on either peaks because of limited statistics.

As a cross-check we analyze the on-resonance data with

the inverted requirement on the normalized Fox-Wolfram moment $R_2 > 0.5$ (Fig. 2 (a), (b)) and off-resonance data sample (Fig. 2 (c), (d)) and find no candidates in the B -signal region. The distributions for the primary vertex protons with an inverted particle identification requirement [32] do not peak in the signal region (Fig. 2 (e), (f)), demonstrating that the selected $\bar{B}^0 \rightarrow D_s^+ \Lambda \bar{p}$ candidates contain real protons.

Table I summarizes the results of the fits, the reconstruction efficiencies including the $\mathcal{B}(D_s^+ \rightarrow \phi \pi^+)$, $\mathcal{B}(\phi \rightarrow K^+ K^-)$, $\mathcal{B}(D_s^+ \rightarrow \bar{K}^{*0} K^+)$, $\mathcal{B}(\bar{K}^{*0} \rightarrow K^- \pi^+)$, $\mathcal{B}(D_s^+ \rightarrow K_S^0 K^+)$, $\mathcal{B}(K_S^0 \rightarrow \pi^+ \pi^-)$, $\mathcal{B}(\Lambda \rightarrow p \pi^-)$ branching fractions, statistical significance of the signals and extracted branching fractions. Here we assume equal fractions of charged and neutral B mesons produced in $\Upsilon(4S)$ decays.

The major sources of systematic error are the uncertainties in the tracking efficiency 6% (1% per track), 12% in the charged particle identification efficiency (1% for pion, 2% for kaon, 3% for proton), 5% for Λ finding, 3% for efficiency estimation due to MC statistics and 5% for the error due to choice of the fitting procedure. These contributions are combined in quadrature resulting in a total systematic error of 16%. We also take into account a third error due to the uncertainty in $\mathcal{B}(D_s^+ \rightarrow \phi \pi^+)$ that is 14%.

In summary, we report the first observation of the decay $\bar{B}^0 \rightarrow D_s^+ \Lambda \bar{p}$ with a branching fraction of $(2.9 \pm 0.7 \pm 0.5 \pm 0.4) \times 10^{-5}$, where the first error is statistical, the second is systematic, and the third arises from uncertainty in the branching fraction of $D_s^+ \rightarrow \phi \pi^+$. The statistical significance is 6.6σ . This charming decay can occur via the creation of an $s\bar{s}$ pair or from the more copious $\bar{B} \rightarrow DN\bar{N}$ modes with $(DN)^+ \rightarrow D_s^+ \Lambda$ rescattering in the final state [5, 7, 33]. In the future, this decay mode can be used for CP asymmetry studies.

We thank the KEKB group for excellent operation of the accelerator, the KEK cryogenics group for efficient solenoid operations, and the KEK computer group and the NII for valuable computing and Super-SINET network support. We acknowledge support from MEXT and JSPS (Japan); ARC and DEST (Australia); NSFC and KIP of CAS (China); DST (India); MOEHRD, KOSEF and KRF (Korea); KBN (Poland); MES and RFAAE (Russia); ARRS (Slovenia); SNSF (Switzerland); NSC

and MOE (Taiwan); and DOE (USA).

-
- [1] Belle Collaboration, N. Gabyshev *et al.*, Phys. Rev. Lett. **90**, 121802 (2003).
- [2] Belle Collaboration, M.-Z. Wang *et al.*, Phys. Rev. Lett. **90**, 201802 (2003).
- [3] Belle Collaboration, K. Abe *et al.*, Phys. Rev. Lett. **88**, 181803 (2002).
- [4] Belle Collaboration, N. Gabyshev *et al.*, Phys. Rev. D **66**, 091102 (2002).
- [5] Belle Collaboration, K. Abe *et al.*, Phys. Rev. Lett. **89**, 151802 (2002).
- [6] CLEO Collaboration, S. A. Dytman *et al.*, Phys. Rev. D **66**, 091101 (2002).
- [7] CLEO Collaboration, S. Anderson *et al.*, Phys. Rev. Lett. **86**, 2732 (2001).
- [8] Belle Collaboration, M.-Z. Wang *et al.*, Phys. Rev. Lett. **92**, 131801 (2004).
- [9] Belle Collaboration, K. S. Park, H. Kichimi *et al.*, Phys. Rev. D **75**, 011101 (2007).
- [10] Belle Collaboration, M.-Z. Wang, Y.-J. Lee *et al.*, Belle preprint 2007-19, arXiv: 0704.2672[hep-ex].
- [11] C.-K. Chua, W.-S. Hou, S.-Y. Tsai, Phys. Rev. D **65**, 034003 (2002).
- [12] C.-K. Chua, W.-S. Hou, S.-Y. Tsai, Phys. Lett. B **528**, 233 (2002).
- [13] J. L. Rosner, Phys. Rev. D **68**, 014004 (2003).
- [14] B. Kerbikov, A. Stavinsky and V. Fedotov, Phys. Rev. C **69**, 055205 (2004).
- [15] J. Haidenbauer, Ulf-G. Meissner and A. Sibirtsev, Phys. Rev. D **74**, 017501 (2006).
- [16] D. R. Entem and F. Fernandez, Phys. Rev. D **75**, 014004 (2007).
- [17] H. Kichimi, Nucl. Phys. B Proc. Suppl. **142**, 197 (2005).
- [18] W.-S. Hou, A. Soni, Phys. Rev. Lett. **86**, 4247 (2001).
- [19] BABAR Collaboration, B. Aubert *et al.*, Phys. Rev. D **72**, 051101 (2005).
- [20] Belle Collaboration, M.-Z. Wang *et al.*, Phys. Lett. B **617**, 141 (2005).
- [21] S. Kurokawa and E. Kikutani, Nucl. Instr. Methods Phys. Res., Sect. A **499**, 1 (2003), and other papers included in this volume.
- [22] Belle Collaboration, A. Abashian *et al.*, Nucl. Instr. Methods Phys. Res., Sect. A **479**, 117 (2002).
- [23] Z. Natkaniec *et al.* (Belle SVD2 Group), Nucl. Instr. and Meth. A **560**, 1 (2006).
- [24] R. Brun *et al.*, GEANT 3.21, CERN DD/EE/84-1, 1984.
- [25] Charged kaons are required to satisfy $\mathcal{L}(K)/(\mathcal{L}(K) + \mathcal{L}(\pi)) > 0.6$. Charged pions are required to satisfy $\mathcal{L}(\pi)/(\mathcal{L}(K) + \mathcal{L}(\pi)) > 0.1$. Protons are required to satisfy $\mathcal{L}(p)/(\mathcal{L}(K) + \mathcal{L}(p)) > 0.6$ and $\mathcal{L}(p)/(\mathcal{L}(\pi) + \mathcal{L}(p)) > 0.6$. Here $\mathcal{L}(K/\pi/p)$ is the particle identification likelihood for the $K/\pi/p$ hypotheses. The above requirements have efficiencies of more than 95% for pions, kaons and protons, respectively, from $\bar{B}^0 \rightarrow D_s^+ \Lambda \bar{p}$ decays. The probability for each particle species to be misidentified as one of the other two is less than 5%.
- [26] W.-M. Yao *et al.*, (Particle Data Group) J. Phys. G **33**, 1 (2006).
- [27] G. C. Fox and S. Wolfram Phys. Rev. Lett. **41**, 1581 (1978).
- [28] Belle Collaboration, S. L. Zang *et al.*, Phys. Rev. D **69**, 017101 (2004).
- [29] Belle Collaboration, N. Gabyshev *et al.*, Phys. Rev. Lett. **97**, 202003 (2006).
- [30] ARGUS Collaboration, H. Albrecht *et al.*, Phys. Lett. B **241**, 278 (1990).
- [31] The B -sideband is defined as a region of $M_{bc} > 5.2 \text{ GeV}/c^2$ and $-0.08 \text{ GeV}/c^2 < \Delta M < 0.12 \text{ GeV}/c^2$ excluding the B -signal region.
- [32] Protons are required to satisfy inverted likelihood ratio requirement $\mathcal{L}(p)/(\mathcal{L}(K) + \mathcal{L}(p)) < 0.6$.
- [33] BABAR Collaboration, B. Aubert *et al.*, Phys. Rev. D **74**, 051101 (2006).